Journal of the Serbian Society for Computational Mechanics / Vol. 16 / No. 2, 2022 / pp 56-66
(10.24874/jsscm.2022.16.02.04)

THE EFFECT OF ROTATION RATES, CYLINDER DIAMETER AND LATERAL BOUNDARIES ON STROUHAL NUMBER IN UNSTEADY REGIMES AT DIFFERENT REYNOLDS NUMBERS

Marouane Essahraoui[1], Rachid El Bouayadi[1], Aouatif Saad[1*]

[1] ASELAB, Advanced Systems Engineering Laboratory, National School of Applied Sciences, Ibn Tofail University, Kenitra, Morocco
e-mail: *saad_aouatif@yahoo.fr, saad.aouatif@uit.ac.ma, marouane.essahraoui@gmail.com*

**corresponding author*

Abstract

The lateral boundary conditions, rotation rates parameters, domain size, cylinder diameter, and Reynolds number are all responsible for the variation of the Strouhal number. In this study, we have varied the domain size, lateral boundary conditions, downstream locations, and the cylinder diameter at specific values of Reynolds number for stationary and rotating cylinders in order to spot the difference in each case. The effect of the rotating cylinder on the flow behavior downstream leads to a variation of Strouhal number. Thus, we have rotated the circular cylinder clockwise and counter-clockwise in order to visualize its effect on the Strouhal number values. An unsteady study was developed for laminar and turbulent regimes from $R_e = 60$ to $R_e = 3900$.

Keywords: unsteady, rotation rates, laminar, turbulent, vortex shedding.

1. Introduction

Investigation of the fluid-structure interactions was the main topic of quite a lot of research, where those interactions create a vortex behind bluff bodies (circular, rectangular and square cylinders). The frequency of some vortex could damage the structure that researchers intend to implement in several applications (submarines, offshore structures, pipelines, etc.). The circular cylinder is a benchmark structure that has been used and studied in the fluid interaction structure. According to recent findings, the domain size, cylinder diameter, rotation rates parameters and lateral boundaries have a critical effect on the behavior of the flow and the variation of fluid parameters (Drag, lift, Strouhal number). Thus, taking into account the placement of the downstream and boundary conditions could help to improve the results and avoid any non-physical integrity.

The two-dimensional numerical study by Tezduyar and Shih (1991) varied the downstream location in unsteady incompressible flow from 2.5 to 25 diameters away from the center of the cylinder at $R_e = 100$. They exhibited that there would be a significant change in the solutions as close as the downstream boundary from the cylinder center. This was also concluded in the studiesd of Braza, Chassaing and Minh (1986), Engelman and Jamnia (1990) and Gerrard (1978).

Another 2-D numerical study by Behr, Hastreiter, Mittal, and Tezduyar (1995) has been investigated. They studied the influence of the lateral boundary, ranging from 9 to 32 diameters away from the cylinder center, where the downstream location was fixed at a specific value; in contrast to the study of Tezduyar & Shih (1991). Their study found that the placement of lateral boundaries influenced the Strouhal number and other quantities such as Drag, lift, etc. Thus, for a better solution, they assumed that the distance between the lateral boundary and cylinder center had to be at least far by eight diameters from the cylinder center.

Several studies have demonstrated that 2-D numerical investigation of incompressible flow around a circular cylinder could provide a significant result only at $R_e < 200$, and for that reason, there is a necessity to use a three-dimensional study in the case of Reynold numbers higher than 200.

Lei, Cheng and Kavanagh (2001) investigated the effect of spanwise length for 2-D and 3-D numerical study from $L_z = 0$ (two-dimensional) to 6 diameters (three-dimensional) at $R_e = 1000$. They concluded the inaccuracy of 2-D simulation at a high value of Reynolds numbers. At the same time, 3-D simulation gave a satisfactory result in a condition of spanwise length that should not be set too small. For $L_z = 0$, the Strouhal number reached a high value of 0.233.

In contrast, for an increased spanwise length, the Strouhal number decreases and remains constant at around 0.20. The results obtained from 3-D simulation agree with the recent experiments' studies. Several studies did not give much attention to the selection of spanwise length and its effect on the variation of fluid parameters quantities, and among these studies we could mention the study of Tamura, Ohta and Kuwahara (1990) who applied a direct finite difference technique to investigate the relation between wake structure and the aerodynamic forces for a spanwise length equal the cylinder diameter in both 2-D and 3-D simulation.

St-Re relationship in an unsteady incompressible flow was the main object of this study at $R_e = 60, 150, 1000, 3900$. We varied the domain size, the cylinder diameter, downstream locations and the lateral boundary for all cases. Also, we studied the effect of CCW and CW rotation rates parameter on the Strouhal number values in a range of $\alpha = -1, -0{,}5, 0.5, 0\ and\ 1$. An unexpected value of $S_{th} = 0.0783$ number appeared for cylinder diameter of (D_1) in the first computational fluid domain at $R_e = 60$, while for the other cases we showed that Strouhal number increased with an increase in Reynolds number and the rotation rates parameter had a slight effect of 0.01 for every case.

2. Numerical Methods

Physical domain

Two-dimensional computational domain has been developed for the simulation of flow around stationary and rotating cylinders. For the first computational domain (Fig. 1), we have set the upstream and downstream 11.5D and 20D, respectively, away from the center of the cylinder and the lateral boundaries 12.5D away from the center of the cylinder, following the study of Behr, Hastreiter, Mittal and Tezduyar (1995), who demonstrated that for better results, we must set lateral boundaries away at least eight diameters from the center of the cylinder. For the second computational domain (Fig. 2), in order to study the effect of lateral boundaries, we have set the upstream and downstream 10D and 40D, respectively, away from the center of the cylinder and the lateral boundaries 6D away from the center of the cylinder. Selection of the computational domain is one of the main concerns facing all researchers where discrepancies in the results appear in an unstable regime. The cylinder rotates by the non-dimensional alpha (Behr, Hastreiter, Mittal, & Tezduyar, 1995) parameter, defined as $\alpha = {}^{\omega D}/_{2U_\infty}$.

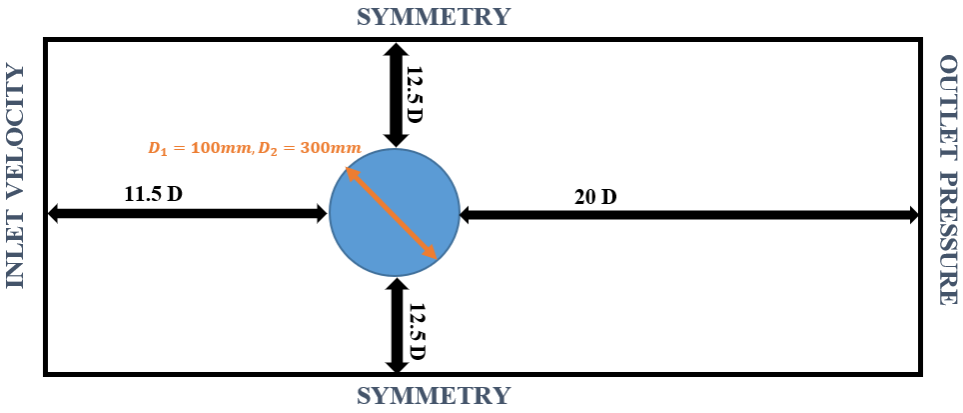

Fig. 1. Computational domain 1.

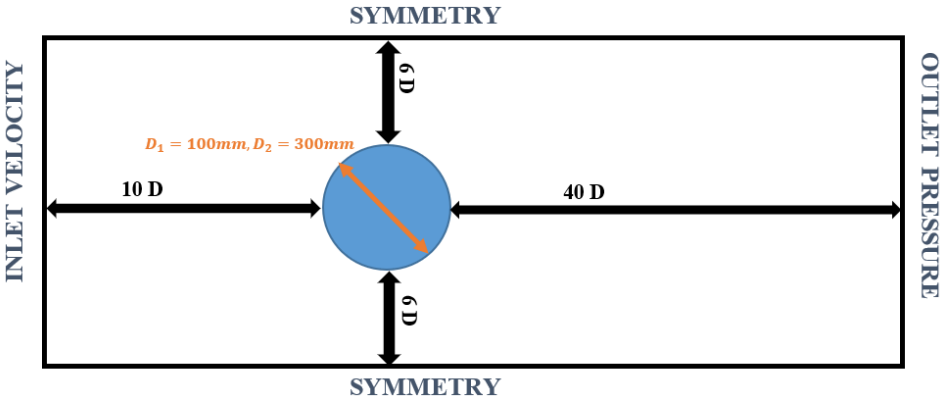

Fig. 2. Computational domain 2.

Fig. 1. shows the first computational domain which is split up into 113100 grid cells and 113910 nodes. Fig. 2 shows the second computational domain which is split up into 87600 grid cells and 8830 nodes. Structured refined mesh has been applied around the cylinders for both computational domain in an attempt to have better accuracy of the results by the CFD solver, and the method used for meshing is the rectangular domain with smooth quadrilateral grids. (Salehi, Mazaheri and Kazeminezhad, 2018).

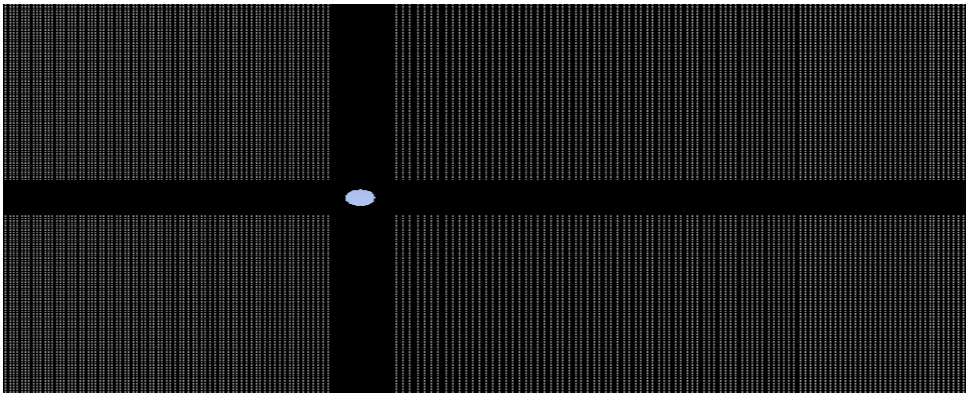

Fig. 3. Grid Computational domain 1.

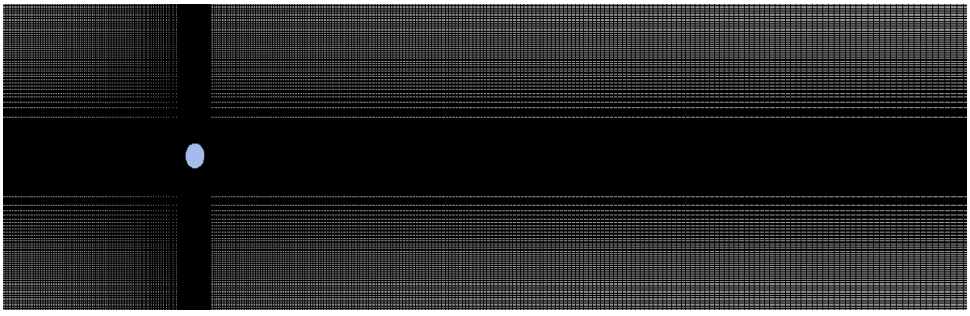

Fig. 4. Grid Computational domain 2.

2.2 Governing equations

Continuity and Navier stoke equations have been used for simulating the incompressible viscous flow. Table 1 represents the continuity equation, the governing equations of unsteady flow, Reynolds's stress tensor, turbulence kinetic energy k, and its dissipation rate ε, respectively (Anderson and John, 1991).

$$\frac{\partial u_i}{\partial x_i} = 0 \tag{1}$$

$$\frac{\partial u_i}{\partial t} + u_j \frac{\partial u_i}{\partial x_j} = -\frac{1}{\rho}\frac{\partial p}{\partial x_i} + \nu \frac{\partial^2 u_i}{\partial x_j^2} - \frac{\partial \overline{u_i' u_j'}}{\partial x_j} \tag{2}$$

$$\overline{-\partial u_i' u_j'} = \nu_T \left(\frac{\partial u_i}{\partial x_j} + \frac{\partial u_j}{\partial x_i}\right) - \frac{2}{3} k \delta_{ij} \tag{3}$$

$$\frac{\partial \rho k}{\partial t} + \frac{\partial \rho k u_i}{\partial x_i} = \frac{\partial}{\partial x_j}\left[\left(\mu + \frac{\mu_T}{\sigma_k}\right)\frac{\partial k}{\partial x_j}\right] + G_k - \rho\varepsilon \tag{4}$$

$$\frac{\partial \rho \varepsilon}{\partial t} + \frac{\partial \rho \varepsilon u_i}{\partial x_i} = \frac{\partial}{\partial x_j}\left[\left(\mu + \frac{\mu_T}{\sigma_\varepsilon}\right)\frac{\partial \varepsilon}{\partial x_j}\right] + C_{1\varepsilon}\frac{\varepsilon}{k}(G_k) - C_{2\varepsilon}\rho\frac{\varepsilon^2}{k} \tag{5}$$

For high Reynolds number, the k-epsilon model has been used to solve the instantaneous Navier-Stokes (N-S) equations (Canbolat, Yıldızeli, Köse, & Çadırcı, 2018). We have used the k-epsilon model for both stationary and rotating cylinders, where k-epsilon can perfectly predict

the flow behavior in such high values of Reynolds number. Strouhal number is a fundamental characteristic parameter of fluid flow, which is defined as follows: $S_{th} = \frac{fD}{U_\infty}$.

Discretization equation

Finite volume method was the method of discretization that was used for this problem. FVM method shows a good accuracy in the case of turbulence problems, where the computational domain splits up into a finite number of elements (Zienkiewicz, Taylor and Nithiarasu, 2014). The FVM is a discretization process that integrates the governing differential equations over each subdomain using a specified integration method, and expresses the results in terms of algebraic quantities which is valid at every grid points. The discretized equation used to convert the general transport equation into an algebraic equation can be written as follows:

$$\frac{\partial \rho \phi}{\partial t} V + \sum_f^{N_{faces}} \rho_f \overrightarrow{v_f} \phi_f . \overrightarrow{A_f} = \sum_f^{N_{faces}} \Gamma_\phi \nabla \phi_f . \overrightarrow{A_f} + S_\phi V \tag{6}$$

Spatial & temporal discretization schemes

Spatial discretization scheme used for dividing the domain into small sub-domain Δx constructing a mesh, in addition the temporal discretization schemes helps to integrate the differential equation over a time step Δt in case of transient simulation. There are various spatial discretization schemes that have been used by several researchers which help finding the face values of variable ϕ and $\nabla \phi_f$ by making assumptions about variation of ϕ between cell centers. In this study, we have applied a Second-order Upwind scheme, which can determine the value of ϕ from the cell values in the two cells upstream of the face and it is one of the most popular numerical schemes because of its combination of accuracy and stability. Thus, the face value ϕ is computed using the following expression (ANSYS, 2009):

$$\phi_f = \phi + \nabla \phi . \vec{r} \tag{7}$$

where ϕ and $\nabla \phi$ are the cell-centered value and its gradient in the upstream cell, and $\vec{r}$ is the displacement vector from the upstream cell centroid to the face centroid (ANSYS, 2009).

The use of temporal discretization is required in the case of transient simulation. In the current study, we have utilized the temporal discretization scheme, which involves the integration of every term in the differential equations over a time step Δt, where the generic expression for the time evolution of a variable ϕ is given by (ANSYS, 2009):

$$\frac{\partial F}{\partial t} = F(\phi) \tag{8}$$

where the function F incorporates any spatial discretization. If the time derivative is discretized using backward differences, the first-order accurate temporal discretization is given by

$$\frac{\phi^{n+1} - \phi^n}{\Delta t} = F(\phi) \tag{9}$$

and the second-order discretization is given by

$$\frac{3\phi^{n+1} - 4\phi^n + \phi^{n-1}}{2\Delta t} = F(\phi) \tag{10}$$

Where n+1, n and n-1 indicative values at time steps $t + \Delta t$, t and $t - \Delta t$ respectively.

3. Results and Discussion

The Strouhal number represents the ratio of the inertial forces due to the local acceleration to the inertial forces due to changes in velocity in the flow field. Due to the unsteadiness of the flow, an oscillating would be generating behind the cylinder causing a vortex shedding phenomenon. The frequency of the vortex could damage every structure under study, because the frequency of vortex shedding generated in the wake is a relevant issue that should be take into consideration. Therefore, we applied a technique that has been used by several authors before, which would serve for calculating the spectral power of power density using a fast Fourier transform (FFT). Researchers have established techniques to determine several factors that are responsible for the variation of Strouhal number. Fluid domain dimension, boundary layer conditions and Reynolds number were one of the substantial factors that lead to a critical variation of Strouhal number. High values of Strouhal number have been reported at critical and super-critical regimes according to Achenbach and Heinecke (1981) and Schewe (1983), where at sub-critical regime the values of Strouhal number remain unchanged up to $R_e = 10^5$ (Williamson, 1996). Furthermore, Reynolds numbers have a substantial effect on the Strouhal number values. In addition, we have endeavored to study the effect of domain size, lateral boundary conditions, rotation rates and Reynolds number in unsteady laminar and turbulent flow regimes for both diameter cylinders to visualize how these parameters affect Strouhal number values. As we showed in the figures that for both cylinder diameter, the influence of the rotation rates has a slightl effect on counter clockwise (CCW) and clockwise (CW) cylinder, and only the increase of Reynolds number who has played a significant rule in the change of Strouhal number values by increasing them with increasing the Reynolds number. The rotation rates influence only in the case when Reynolds equal 60, where the Strouhal number increase for both rotating cylinder diameter 0.2 up to the value of stationary cylinder. For unsteady laminar flow and in the case of Re number equaling 60, the rotation rates could have an impact by increasing the frequency of the oscillating fluid flow.

3.1 Strouhal number for unsteady laminar and turbulent regimes

We will exhibit the variation of Strouhal number in the case of stationary and rotating circular cylinder for both domain size, lateral boundaries, downstream location and different cylinder diameter. First, we will consider the variation of Strouhal number at various Reynolds numbers for both different cylinder diameters, lateral boundaries, downstream location and domain size in stationary case. Tables 2 and 3 show the values of Strouhal number for both domain sizes.

3.2 Stationary circular cylinder

In the case of domain size 1 (Table 2), we can clearly see the augmentation of Strouhal number with every increase of Reynolds numbers for both regimes, and the values of Strouhal number are closely akin at each value of Reynolds numbers with a small difference at $R_e = 3900$ for both cylinders diameter. Furthermore, a large computational domain with a lateral boundary set far from the cylinder center would lead to a reasonable result according to several studies.

	STROUHAL NUMBER VALUES			
	$R_e = 60$	$R_e = 150$	$R_e = 1000$	$R_e = 3900$
$D_1 = 100mm$	0.123	0.178	0.192	0.232
$D_2 = 300mm$	0.123	0.179	0.192	0.224

Table 1. S_{th} for both cylinders diameter domain size 1.

In the case of domain size 2, we can see some discrepancies in the results, where the values of Strouhal number are not the same for both cylinders diameters, and the Strouhal number values increased and decreased at each value of Reynolds number. In the case of cylinder diameter D1 and at $R_e = 60$ a noticeable value of Strouhal number appeared, where the value of Strouhal number decreased to a small value $S_{th} = 0.0783$ compared to the same value of Reynolds number of the domain size 1, which indicates that the frequency of vortex is too small. According to Behr, Hastreiter, Mittal and Tezduyar (1995), we can conclude that influence on the results in the case of domain size 2 is induced by the set of lateral boundaries, which are close from the cylinder center. Furthermore, the influence of lateral boundaries was obvious for both cases, and gave us a sufficient idea about the effect of lateral boundaries on the results. The way we set the lateral boundary conditions, upstream and downstream locations have a critical effect on the final results. As we can see from Table 1, cylinder diameter has no significant effect if the fluid domain used was large enough, and the variation of Strouhal number depends only on the Reynolds number. In contrast, in Table 2, cylinder diameter plays a critical role defining the variation of Strouhal number at $R_e = 60$, where the value of Strouhal number has a noticeable change and ranging from small value to a high value. Furthermore, for a small fluid domain the values of Strouhal number undergo some discrepancies.

	STROUHAL NUMBER VALUES			
	$R_e = 60$	$R_e = 150$	$R_e = 1000$	$R_e = 3900$
$D_1 = 100mm$	0.0783	0.153	0.192	0.224
$D_2 = 300mm$	0.134	0.185	0.184	0.208

Table 2. S_{th} for both cylinders diameter domain size 2.

3.3 Rotating circular cylinder

In the case of rotating cylinders, we have rotated the cylinders CCW (counter-clockwise) and CW (clockwise) to study their effect on the variation of Strouhal number compared to the stationary cylinders. Figures below depicted the variation of Strouhal number for both domain size in a range of $\alpha = -1, -0{,}5, 0.5, 0\ and\ 1$. Figures 5 and 6 show the comparison between rotating and stationary cylinders in the case of domain size 1, where the values of Strouhal number CCW and CW remain the same, and the values of Strouhal number increased compared to the stationary cylinders at Re=60. Furthermore, rotating cylinders in a sizeable fluid domain have no significant effect on the results, where the only parameter responsible for the change of the Strouhal number values was the Reynolds number.

Slight variation between CCW (counter-clockwise) and CW (clockwise) rotating cylinders in the case of domain size 2 appeared for cylinder diameter D1, but when we compared between rotating and stationary cylinder we could visualize some discrepancies in the results, since the values that we found for rotating cylinder are larger than the stationary cylinder in the case of D1 domain size 2.

According to several studies, which investigated the effect of domain size, downstream location and lateral boundaries, it was found that lateral boundaries had a noticeable effect on the fluid flow parameters such as Strouhal number. In our study, we conclude that the lateral boundaries that we have applied in the case of domain size 2 influence the values of Strouhal number, and especially in the case of stationary cylinder at Re=60.

In the figures below, the positive α values correspond to (CCW) counter-clockwise rotation, whereas the negative α values correspond to (CW) clockwise rotation. $\alpha = 0$ indicates a stationary circular cylinder case for both diameters.

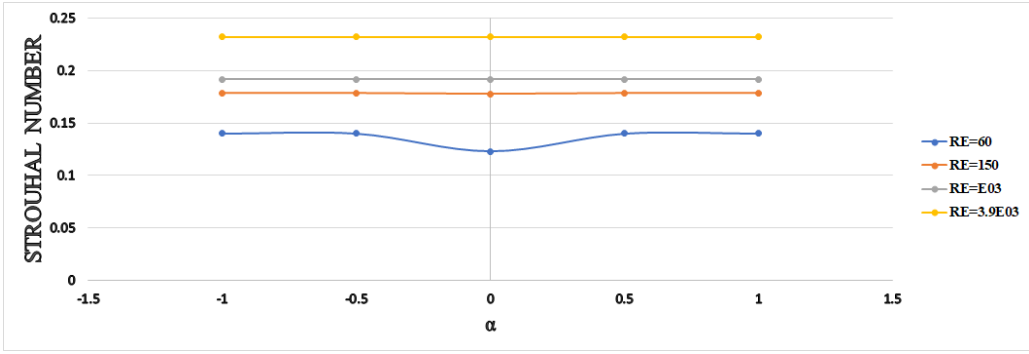

Fig. 5. S_{th} for cylinder diameter D1 at various value of Reynolds number and rotation rates parameters domain size 1.

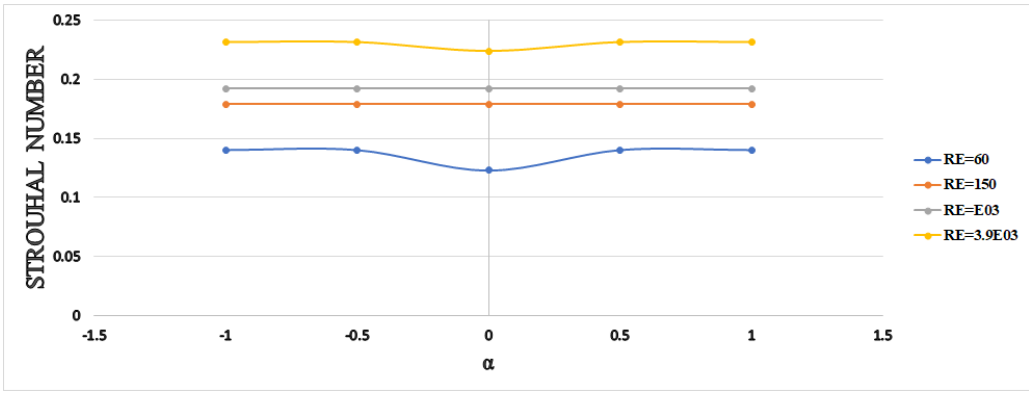

Fig. 6. S_{th} for cylinder diameter D2 at various value of Reynolds number and rotation rates parameters domain size 1.

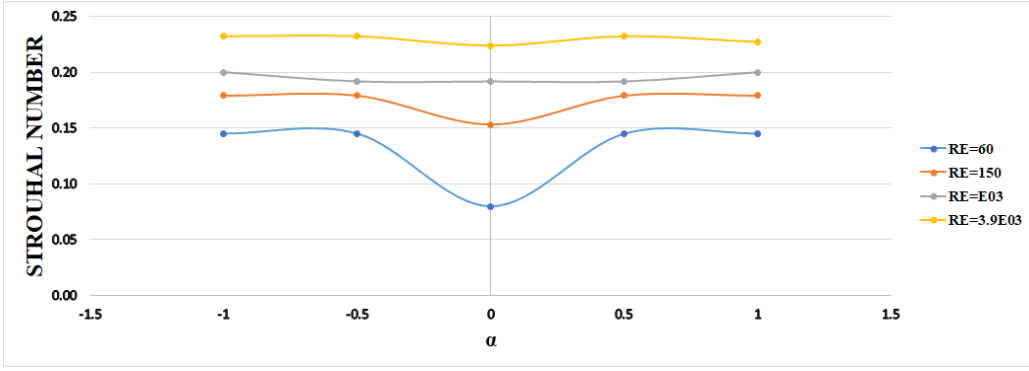

Fig. 7. S_{th} for cylinder diameter D1 at various value of Reynolds number and rotation rates parameters domain size 2.

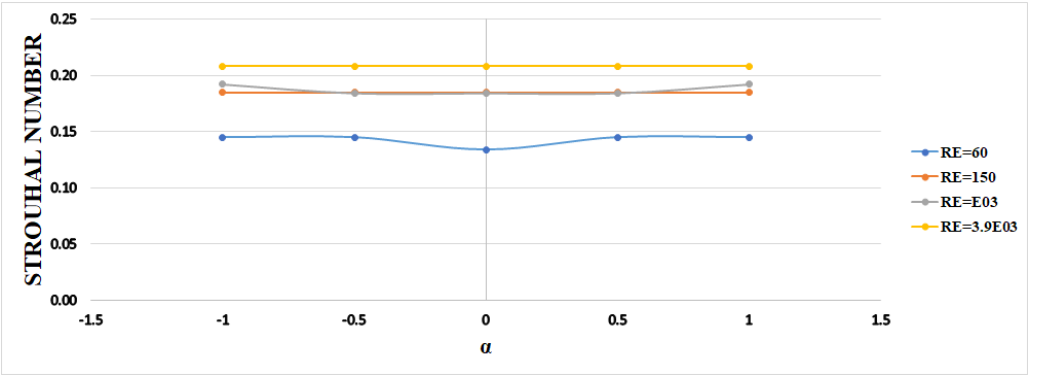

Fig. 8. S_{th} for cylinder diameter D2 at various value of Reynolds number and rotation rates parameters domain size 2.

4. Conclusions

In this numerical study, we have investigated the influence of the domain size, cylinder diameter, the position of lateral boundaries and downstream from the cylinder center at various Reynolds numbers and rotation rates parameters on the Strouhal numbers values. Both circular cylinders with different diameters are placed in a large and small domain size. In the first test, we have studied the variation of Strouhal number in the case where the circular cylinder is stationary for both domain sizes at various Reynolds numbers. Furthermore, we concluded that the values of Strouhal number increased with every increase of Reynolds numbers, and the values are similar for both cylinder diameter and domain size. All these results lead us to the major conclusion that when the domain size is large and the lateral boundaries are placed far away from the circular cylinder, the Strouhal number values are consistent with recent findings. For the second test, we have set the lateral boundaries so close to the cylinder center, which induced a scattering result especially in the case of cylinder diameter D1, where the values of Strouhal number were not similar compared to the first test, and the value of Strouhal number decreased to a small value of 0.783 in the range of rotation rates parameters that we have applied on the circular cylinder, we can see clearly no impact of that parameters on the values of drag compared to the stationary circular cylinder. Thus, the only changes happened in the case of domain size 2 of cylinder diameter D1, where the values of Strouhal number were high compared to the case of rotating cylinder. Conclusions may thus be reached regarding the effect of domain size and lateral boundaries on the values of the Strouhal number under various regimes for both cylinder diameters. Furthermore, additional study may be undertaken utilizing several turbulence models (DNS, LES, etc.) to see how these models may affect the results. In addition, we may transition to a 3D simulation in an effort to gain a comprehensive understanding of the Strouhal number and prevent damage caused by the frequency of particular vortices.

Nomenclature

x_i	Cartesian coordinates
u_1, u_2	Mean velocity components of the fluid in x, and y directions respectively
$\overline{u_i' u_j'}$	Reynolds stress components

u_i'	Fluctuating part of the velocity
p	The dynamic pressure
ρ	The density of the fluid
k	The turbulent kinetic energy
ε	The dissipation rate
ν_T	Turbulent viscosity $\nu_T = C_\mu \frac{k^2}{\varepsilon}$
G_k	Generation of turbulence kinetic energy due to the mean velocity gradients
$C_{1\varepsilon}, C_{2\varepsilon}$	Empirical model coefficients vary depending of the k-epsilon model
$\sigma_{k,}\sigma_\varepsilon$	Turbulent Prandtl number for $k\ and\ \varepsilon$
ω	The angular rotational speed
U_∞	The uniform velocity inlet
D	Diameter of the cylinder
α	Non-dimensional rotational parameter
f	Vortex shedding frequency
N_{faces}	Number of faces enclosing cell
ϕ_f	Value of ϕ convicted through face f
$\rho_f \overrightarrow{v_f}.\overrightarrow{A_f}$	Mass flux through the face
$\overrightarrow{A_f}$	Area of face f, $\lvert A\rvert$ $(= \left\lvert A_x\hat{\imath} + A_y\hat{\jmath}\right\rvert\ in\ 2D)$
$\nabla\phi_f$	Gradient of ϕ at face f
V	Cell volume
Γ_ϕ	Diffusion coefficient for ϕ
S_ϕ	Source of ϕ per unit volume
ϕ	Scalar quantity
R_e	Reynolds number

References

Achenbach E and Heinecke E (1981). On vortex shedding from smooth and rough cylinders in the range of Reynolds numbers 6× 103 to 5× 106. *Journal of Fluid Mechanics*, 239-251.

Anderson and John D (1991). *Fundamentals of Aerodynamics, 2nd Edition.* New York: McGraw-Hill.

ANSYS. (2009). *ANSYS.* Retrieved from www.afs.enea.it: https://www.afs.enea.it/project/neptunius/docs/fluent/html/th/node366.htm

Behr M, Hastreiter D, Mittal S, and Tezduyar TE (1995). Incompressible flow past a circular cylinder: dependence of the computed flow field on the location of the lateral boundaries. *Computer Methods in Applied Mechanics and Engineering*, 309-316.

Braza M, Chassaing P H, and Minh HH (1986). Numerical study and physical analysis of the pressure and velocity fields in the near wake of a circular cylinder. *Journal of Fluid Mechanics*, 79-130.

Canbolat G, Yıldızeli A, Köse HA, and Çadırcı S (2018). Numerical Investigation of Transitional Flow over a Flat Plate under Constant Heat Fluxes. *Academic Perspective Procedia*, 187-195.

Engelman MS, and Jamnia M A(1990). ransient flow past a circular cylinder: a benchmark solution. *International Journal for Numerical Methods in Fluids*, 985-1000.

Gerrard J H (1978). The wakes of cylindrical bluff bodies at low Reynolds number. *Philosophical Transactions of the Royal Society of London. Series A, Mathematical and Physical Sciences*, 351-382.

Gioria R S, Meneghin JR, Aranha JA, Barbeiro I C, and Carmo B S (2011). Effect of the domain spanwise periodic length on the flow around a circular cylinder. *Journal of Fluids and Structures*, 792-797.

Lei C, Cheng L, and Kavanagh K (2001). Spanwise length effects on three-dimensional modelling of flow over a circular cylinder. *Computer Methods in Applied Mechanics and Engineering*, 2909-2923.

Salehi M A, Mazaheri S, and Kazeminezhad M H (2018). Study of Flow Characteristics Around a Near-Wall Circulair Cylinder Subjected to a Steady Cross-Flow. *International Journal of Coastal & Offshore Engineering*, 45-55.

Schewe G (1983). On the force fluctuations acting on a circular cylinder in crossflow from subcritical up to transcritical Reynolds numbers. *Journal of Fluid Mechanics*, 265-285.

Tamura T, Ohta I, and Kuwahara K (1990). On the reliability of two-dimensional simulation for unsteady flows around a cylinder-type structure. *Journal of Wind Engineering and Industrial Aerodynamics*, 275-298.

Tezduyar T E, and Shih R (1991). Numerical experiments on downstream boundary of flow past cylinder. *Journal of Engineering Mechanics*, 854-871.

Williamson C H (1996). Vortex dynamics in the cylinder wake. *Annual Review of Fluid Mechanics*, 477–539.

Zienkiewicz OC, Taylor R L, and Nithiarasu P (2014). *The Finite Element Method for Fluid Dynamics.* Elsevier BV 1.